Steel and Composite Structures, Vol. 6, No. 6 (2006) 479-491
DOI: http://dx.doi.org/10.12989/scs.2006.6.6.479

Identifying the hysteretic energy demand and distribution in regular steel frames

Bulent Akbas†

Department of Earthquake and Structural Science, Gebze Institute of Technology, 41400 Gebze-Kocaeli, Turkey

Jay Shen‡

Department of Civil and Architectural Engineering, Illinois Institute of Technology, 60616-3793 Chicago, IL, USA

Hakan Temiz‡†

Department of Earthquake and Structural Science, Gebze Institute of Technology, 41400 Gebze-Kocaeli, Turkey

(Received July 20, 2005, Accepted June 15, 2006)

Abstract. Structures in seismic regions are designed to dissipate seismic energy input through inelastic deformations. Structural or component failure occurs when the hysteretic energy demand for a structure or component subject to an earthquake ground motion (EQGM) exceeds its hysteretic energy dissipation capacity. This paper presents a study on identifying the hysteretic energy demand and distribution throughout the height of regular steel moment resisting frames (SMRFs) subject to severe EQGMs. For this purpose, non-linear dynamic time history (NDTH) analyses were carried out on regular low-, medium-, and high-rise steel SMRFs. An ensemble of ninety EQGMs recorded on different soil types was used in the study. The results show that the hysteretic energy demand decreases from the bottom stories to the upper stories and for high-rise structures, most of the hysteretic energy is dissipated by the bottom stories. The decrease is quite significant, especially, for medium- and high-rise structures.

Keywords: energy input; hysteretic energy; steel frames; non-linear analysis.

1. Introduction

Structures in seismic regions are designed to dissipate seismic energy input through inelastic deformations. Structural or component failure occurs when the hysteretic energy demand for a structure or component subject to an earthquake ground motion (EQGM) exceeds its hysteretic energy dissipation capacity. Energy input (E_I) is partly dissipated by hysteretic energy (E_H) through hysteretic behavior. That is why

†Assistant Professor, Corresponding author, E-mail: akbasb@gyte.edu.tr
‡Associate Professor
‡†Research Assistant

E_H can be used as a seismic design parameter when the damage is expected not to exceed some specified limits (Bertero and Teran-Gilmore 1994). For certain performance levels, hysteretic energy can be used as a limiting value in earthquake-resistant design such as drift, ductility, structural damage and storey drift indices, etc. (Vision-2000 1995, Bertero and Bertero 1999).

Housner (1956) first introduced the energy concept into seismic response of single-degree-of-freedom (SDOF) systems. The studies on the energy concept have mainly concentrated on SDOF systems (Zahrah and Hall 1984, Akiyama 1985, Fajfar and Vidic 1989, Kuwamura and Galambos 1989, Uang and Bertero 1990, Bruneau and Wang 1996). However, the inelastic seismic behavior of multi-degree-of-freedom (MDOF) and SDOF systems may differ dramatically. SDOF systems have limitations when used to determine the energy values in MDOF systems due to two main reasons: a) they may underestimate the energy input on high-rise structures due to the contribution of higher modes, which may become important for earthquake ground motions having high frequency content (Bertero and Teran-Gilmore 1994); b) hysteretic energy is the main cause of the plastic deformation of structural members and its distribution depends on the structural systems, which are MDOF systems, as much as on the ground motion.

Akiyama (1985) developed Housner's (1956) method and devised an earthquake-resistant design method which can be applied in a uniform manner to one-story buildings through high-rise buildings. Kuvamura *et al.* (1992) studied the prediction of earthquake energy input of damped elastic SDOF systems from smoothed fourier amplitude spectrum. Their study has shown that the increase in damping factor results in a more smoothed spectrum in SDOF systems, but smoothing effects due to higher mode participation is less significant than the smoothing effect due to damping in MDOF systems due to the predominant first mode participation. Tso *et al.* (1993) studied equivalent SDOF systems to estimate the input and hysteretic energy demands on low-rise ductile moment-resisting buildings. They have concluded that for high-rise ductile moment-resisting buildings, higher modal responses become significant and the use of equivalent SDOF systems may underestimate the energy demands on buildings. This is particularly true for earthquake ground motions having relatively high frequency content, which increases the higher modal contributions. Shen and Akbas (1999) predicted the energy input in low-, medium-, and high-rise steel moment resisting frames (SMRFs) and proposed an energy-based earthquake resisting design method. In their study, they made comparisons of the energy input with the formulas proposed for mainly SDOF systems and concluded that there was a clear difference between the SDOF and MDOF systems in terms of energy input. Reyes-Salazar and Haldar (2001a, b) studied analytically the energy dissipation in steel frames with partially restrained connections subject to earthquake loading. They carried out non-linear dynamic time history analyses on 1-, 3-, and 8-storey steel frames and found out that partially restrained connections were a major source of energy dissipation, even though they reduced the overall stiffness of the structure. In another study by the same authors (2000), they tried to verify the mathematical model using experimental results, for two loading conditions. They observed that as the connections became stiffer, the less energy was dissipated by the connection. Choi (2004) investigated the hysteretic energy input characteristics, plastic rotation distributions, and storey drift ratios on 16-storey high-rise SMRFs with mass and stiffness irregularities.

This paper presents a study on identifying the hysteretic energy distribution throughout the height of regular steel moment resisting frames (SMRFs) subject to severe EQGMs. For this purpose, non-linear dynamic time history (NDTH) analyses were carried out on regular low-, medium-, and high-rise steel SMRFs. EQGMs used in this study were recorded on different soil types. The results are presented in terms of the hysteretic energy distribution with respect to the soil type and earthquake intensity.

2. Energy response of inelastic systems

The energy input into an inelastic system due to an EQGM is dissipated by both viscous damping and yielding. The following energy terms can be defined by integrating the equation of motion as follows (Chopra 2000):

$$\int_0^u m\ddot{u}(t)du + \int_0^u c\dot{u}(t)du + \int_0^u f_s(u, \dot{u})du = -\int_0^u m\ddot{u}_g(t)du \tag{1}$$

where m is the mass; c is the viscous damping coefficient, f_s is the restoring force (for a linear elastic system $f_s = ku$, k = rigidity), u is the relative displacement of the mass relative to the ground, u_g is the earthquake ground motion displacement. The right side of Eq. (1) represents the seismic energy input, E_I, to the structure. $E_I(t)$ is defined as the work done by the effective seismic force (the mass times ground acceleration) over the structural deformation.

$$E_I(t) = -\int_0^u m\ddot{u}_g(t)du \tag{2}$$

The first term on the left side of Eq. (1) is the kinetic energy, E_k. $E_k(t)$ is proportional to relative velocities of masses at time t, which is only related to the instant response of the structure at time t and can be found by multiplying half of the mass with its motion relative to the ground as follows:

$$E_k(t) = \int_0^u m\ddot{u}(t)du = \int_0^u m\dot{u}(t)d\dot{u} = \frac{m\dot{u}^2}{2} \tag{3}$$

The second term on the left side of Eq. (1) is the damping energy, E_D. $E_D(t)$ is physically interpreted as the energy dissipated by the viscous damping of the system and a cumulative quantity, ever increasing with the time during the vibration.

$$E_D(t) = \int_0^u f_D(t)du = \int_0^u c\dot{u}(t)du \tag{4}$$

The third term on the left side of Eq. (1) is the sum of the hysteretic energy, E_H, and the elastic strain energy, E_e. $E_e(t)$ is an instant quantity depending on the current elastic deformation level at time t.

$$E_e(t) = \frac{[f_S(t)]^2}{2k} \tag{5}$$

where k is the initial stiffness of the system. $E_H(t)$ is a cumulative quantity over the plastic deformation throughout the entire duration of the vibration, and will be zero if the structure remains elastic.

$$E_H(t) = \int_0^u f_S(u, \dot{u})du - E_e(t) \tag{6}$$

E_H includes the inelastic deformation of structural members and is directly related to the cyclic deformation capacity of structural components. In an elastic response, E_H is equal to zero, whereas E_e is negligible compared to E_H in an inelastic response. At any instant time t, E_k and E_e can be computed from Eqs. (3) and (5), respectively. Thus, the energy response terms of a non-linear system can be written as:

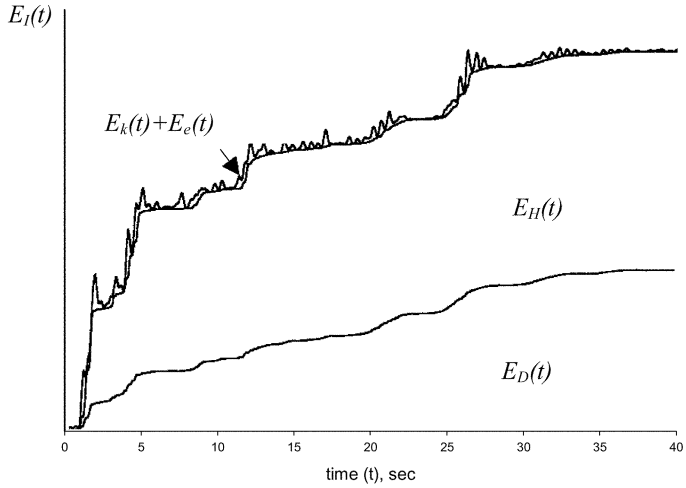

Fig. 1 Energy response terms

$$E_k(t) + E_D(t) + E_e(t) + E_H(t) = E_I(t) \tag{7}$$

If Eq. (7) were considered as a design equation (demand ≤ capacity), the four terms on the left-hand side of Eq. (7) could be considered as energy response of the structure (capacity) and the term on the right-hand side as energy input (demand). Fig. 1 shows a typical energy response of a non-linear system. The instant kinetic energy and elastic strain energy consist of relatively small portion of the E_I at any time during the vibration and vanish at the end of the vibration. The E_D and E_H, therefore, are major contributors for dissipating the E_I. Thus, E_k and E_e are negligible in an inelastic response and Eq. (7) can be practically written as:

$$E_D + E_H = E_I \tag{8}$$

For a given structure and EQGM, the quantities in Eq. (8) at the end of the EQGM can be determined and the distribution of hysteretic energy throughout the structure can be evaluated.

3. Identifying hysteretic energy demand in steel moment resisting frames

3.1. Nonlinear dynamic history analyses

Energy response analyses through NDTH analyses were carried out on three steel buildings with 3-, 9-, and 20-stories. These buildings were designed for gravity, wind, and seismic loads as part of the SAC Steel Project and represent typical low-, medium-, and high-rise steel buildings (Ohtori *et al.* 2000). The structural system for all buildings consisted of steel moment resisting perimeter frames and interior simply connected frames for gravity, i.e., lateral loads were carried by the perimeter frames. The elevation of the perimeter frames to carry lateral loads are given in Fig. 2.

The frames were modeled by DRAIN-2DX (Prakash *et al.* 1993). The two-dimensional models of the frames were built for NDTH analyses. Beam-column elements were used in the analyses and inelastic

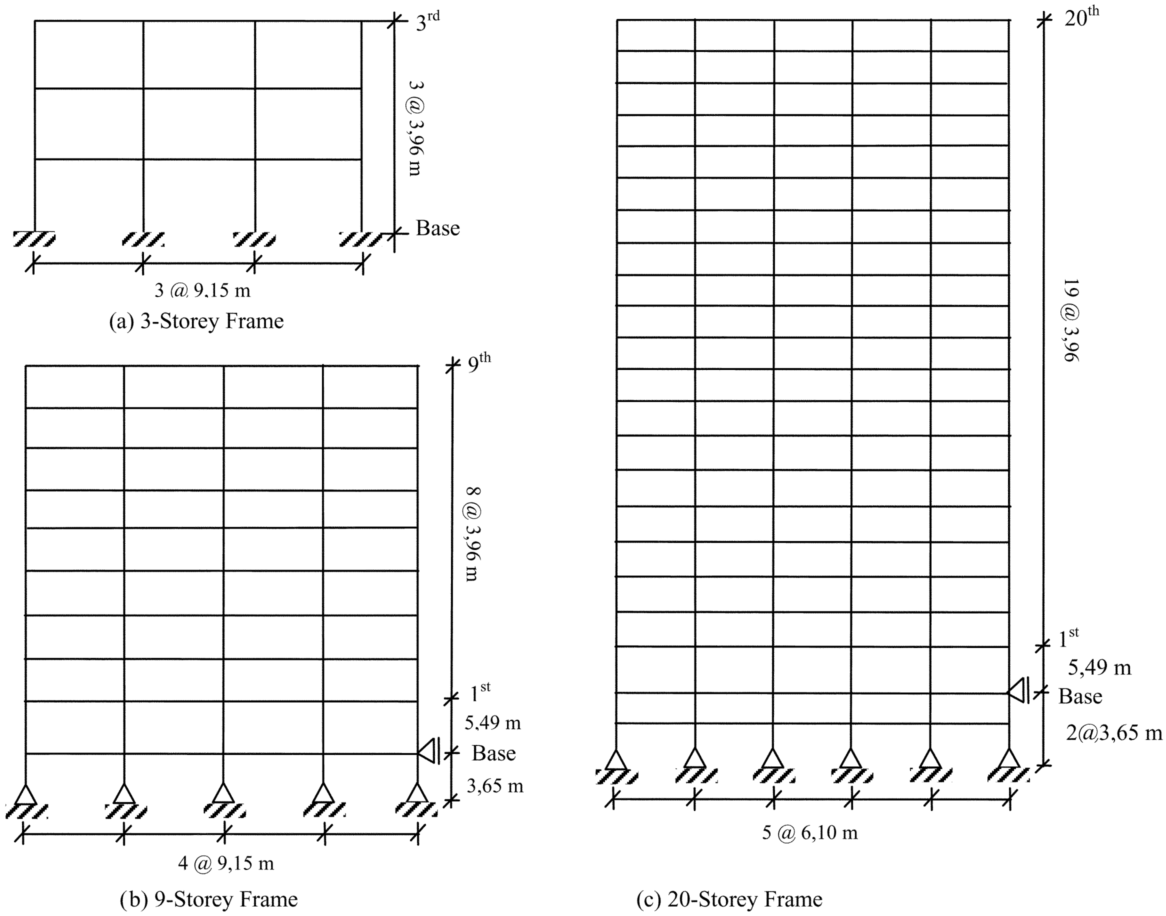

Fig. 2 Elevation of the frames

effects were assigned to plastic hinges at the member ends. The bilinear inelastic behavior was assumed with a strain hardening of 5% of the initial stiffness in all elements. A stable cyclic deformation was assumed. Mass was assumed to be lumped at the joints. Damping ratio was assumed to be 5%. Since either of the mass- or stiffness-proportional dampings provides the same damping ratios for higher modes, Rayleigh damping was used in the analyses. Rayleigh damping expresses the damping matrix as a linear combination of mass and stiffness matrices (Chopra 2000). In practice, the modes i and j are chosen in such a way that higher modes will result in somewhat close damping ratios and contribute to the response. In this study, Rayleigh damping with the first and third, second and fourth, and third and sixth natural frequencies for the 3-, 9-, and 20-storey frames, respectively, was used in the analyses. *P-M* (axial load-moment) interaction relation, suggested by AISC-LRFD (1999), was used as yielding surface of column elements. Beams were modeled as flexural elements. The panel zone effect was neglected in the analyses, but large deformation (P-Δ) effect was considered on the analyses of 9- and 20-storey frames. The seismic masses of the buildings were 2950 t, 9000 t, and 11100 t for 3-, 9-, and 20-storey buildings, respectively. The first natural periods of the 3-, 9-, and 20-storey frames were 1.0109 sec, 2.2862 sec, and 3.7863 sec, respectively. For NDTH analyses, an ensemble of 90 EQGMs recorded on

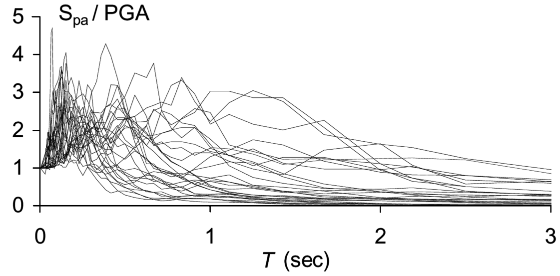

(a) *Type A&B*

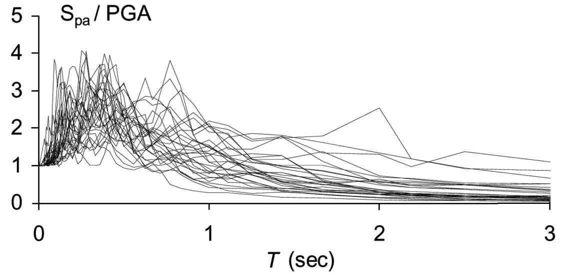

(b) *Type C*

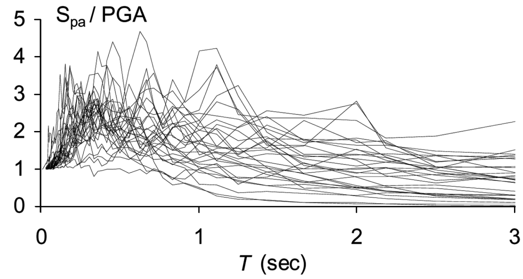

(c) *Type D*

Fig. 3 The normalized response spectra

four different soil types (*Type A, B, C* and *D*) were used in the study. Soil types in which shear velocities (V_s) are bigger than 750 m/sec, between 360-750 m/sec, 180-360 m/sec and less than 180 m/sec, are defined as *Type A*, *B*, *C* and *D* (http://peer.berkeley.edu/smcat/sites.html), respectively. The EQGMs were grouped with respect to the soil type as *Type A&B*, *Type C* and *Type D* each having 30 records making a total of 90. Detailed information about the EQGMs can be found at Sari (2003). The EQGMs were recorded during 20 earthquakes from all over the world (Imperial Valley 1979, Loma Prieta 1989, Kobe 1995, Kocaeli 1999, Chi-Chi 1999, etc.). The peak ground accelerations (PGAs) are varying between 0.01 and 0.69 g, where g is acceleration due to gravity. The closest distances for the records vary from 0.3 to 217 km. The site classes and corresponding shear wave velocities refer to over the top 30 m of the soil layer. The PGA of the EQGMs was scaled to 0.4 g, 0.6 g, and 0.8 g to investigate the frames' seismic responses under severe EQGMs. The normalized response spectra of the EQGMs are given in Fig. 3. Each frame was subjected to the EQGMs in each soil type group. A total of 810 NDTH analyses were carried out.

3.2. Results and discussion

The results obtained from the NDTH analyses were presented in the form of the distribution of the hysteretic energy demand throughout the height of the frames with respect to soil type and EQ intensity. E_H will be mostly dissipated by the steel beams in a code-designed building considering strong column-weak beam requirement. Strong column-weak beam requirement was observed to be strictly imposed to avoid early inelastic deformation in the columns in the design of the frames. The results of the E_H demand only on the beams ($E_{H,beams}$) and on the beams + columns ($E_{H,beams+columns}$) at the storey levels are given in Figs. 4, 5, and 6 for 3-, 9-, and 20-storey frames, respectively. In the Figs., the E_H demands

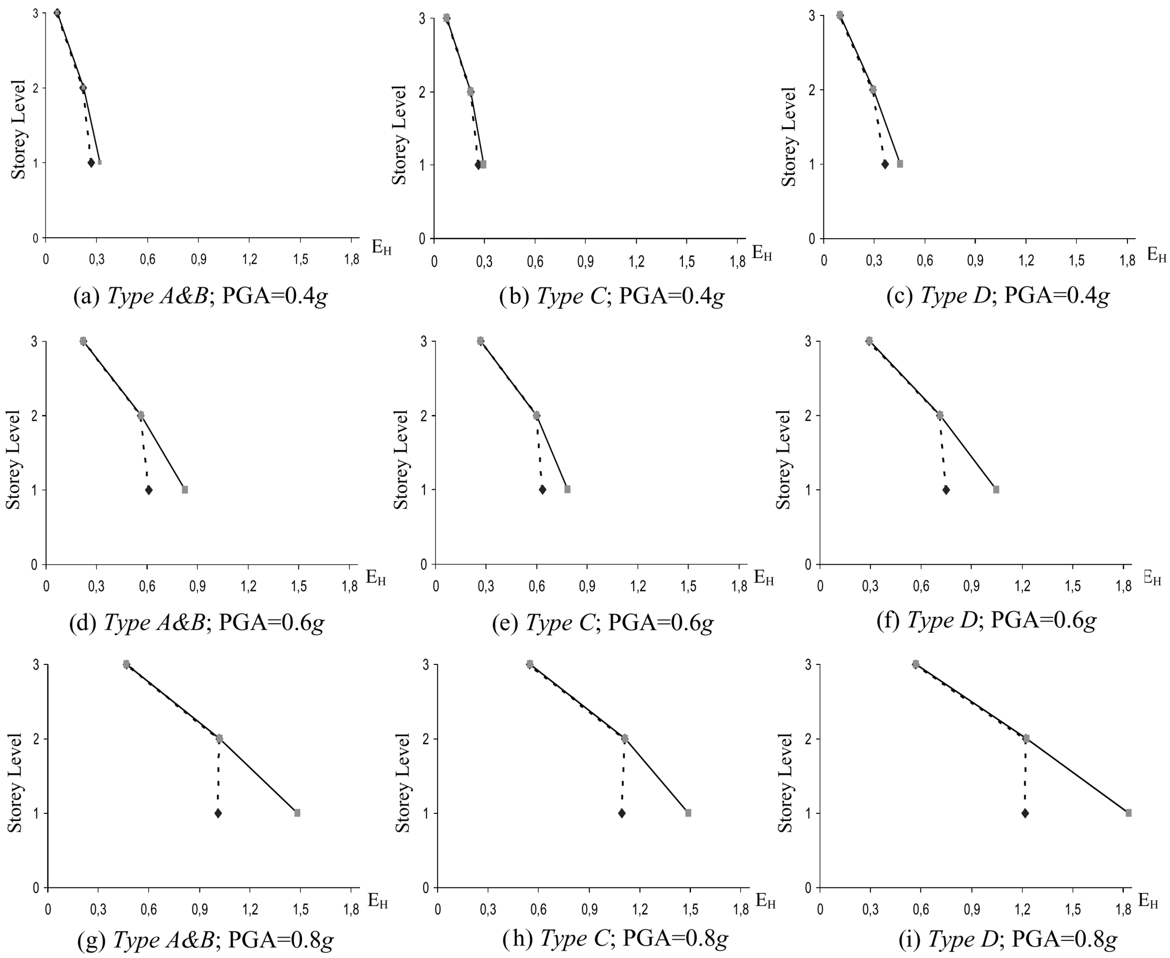

(a) *Type A&B*; PGA=0.4*g* (b) *Type C*; PGA=0.4*g* (c) *Type D*; PGA=0.4*g*

(d) *Type A&B*; PGA=0.6*g* (e) *Type C*; PGA=0.6*g* (f) *Type D*; PGA=0.6*g*

(g) *Type A&B*; PGA=0.8*g* (h) *Type C*; PGA=0.8*g* (i) *Type D*; PGA=0.8*g*

Fig. 4 Distribution of hysteretic energy for the 3-storey frame, Nm × 10^6 (------- $E_{H,beams}$, ——— $E_{H,beams+columns}$)

at the storey levels represent the mean of the 30 NDTH analyses results for the specific soil type.

Figs. 4, 5, and 6 clearly show the difference between the $E_{H,beams}$ and $E_{H,beams+columns}$. For PGA=0.4 g, 0.6 g, and 0.8 g, almost all the E_H was dissipated by the beams for any soil type for the 3- and 9-storey frames. The difference at the first storey was due to the E_H being dissipated through the base of the frames (Figs. 4(a) through (i) and Figs. 5(a) through (i)). However, for the 20-storey frame, the E_H demand also occurred significantly at the columns for PGA=0.4 g, 0.6 g, and 0.8 g.

Table 1 shows the $E_{H,beams}$ to $E_{H,beams+columns}$ ratio by at each storey of the 3-storey frame. The lowest $E_{H,beams}$ to $E_{H,beams+columns}$ ratio was 0.66 on Type D for PGA=0.8 g at the first storey. This ratio was in the range of 0.66 and 0.89 at the first storey and tended to decrease as the EQ intensity increased. At the second and third stories, this ratio was almost equal to 1.00, meaning that there was no E_H demand by the columns of those stories and all the E_H was dissipated by the beams. In overall, this ratio varied from 0.83 to 0.94 for the 3-storey frame. This should not let misinterpret the results, because for the 3-storey frame, only the base of the first storey columns dissipated the E_H, and the columns at the other stories did not go beyond elastic range. This ratio was the highest for *Type C*, while it was the lowest for *Type D* for any EQ intensity.

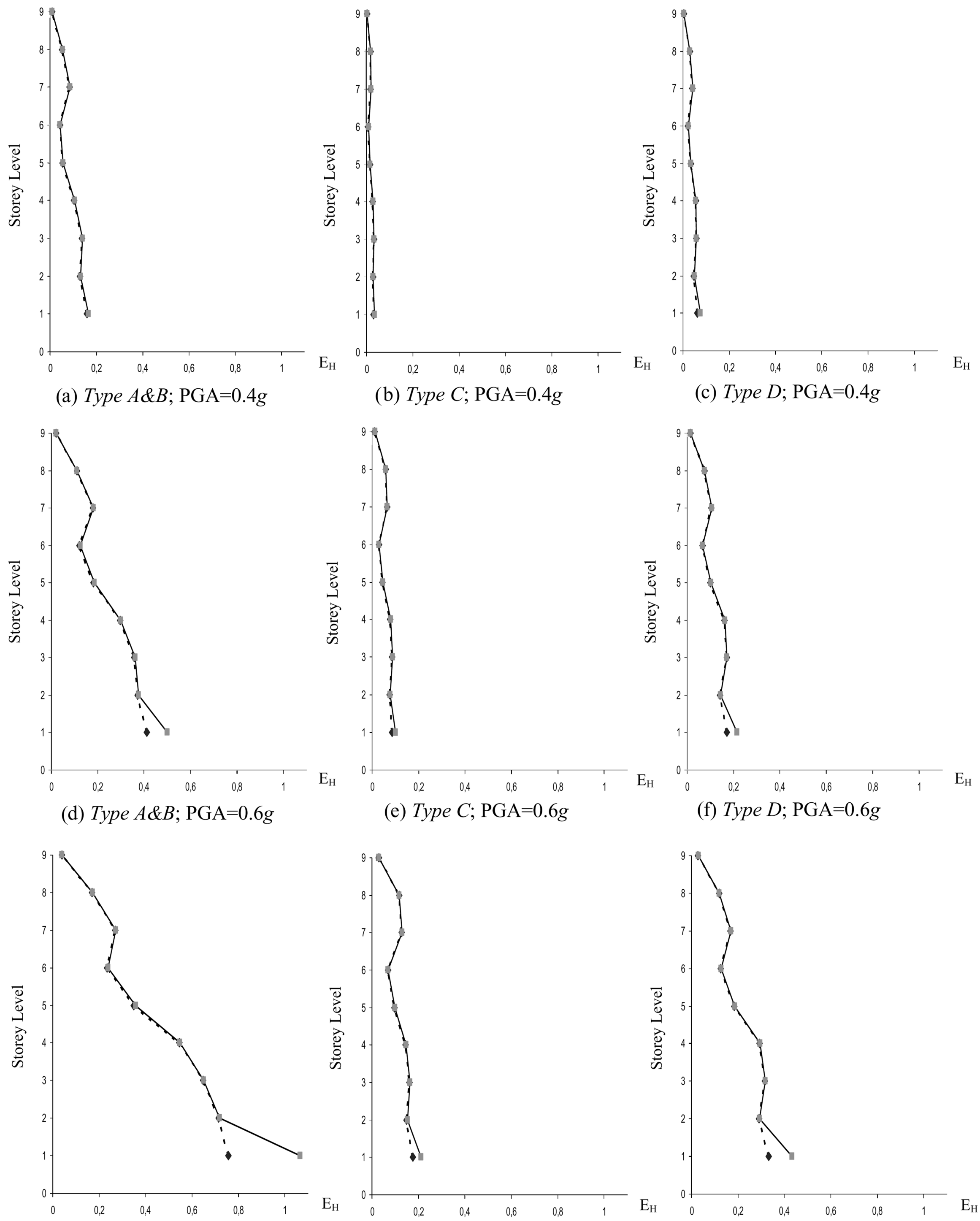

(a) *Type A&B*; PGA=0.4*g* (b) *Type C*; PGA=0.4*g* (c) *Type D*; PGA=0.4*g*

(d) *Type A&B*; PGA=0.6*g* (e) *Type C*; PGA=0.6*g* (f) *Type D*; PGA=0.6*g*

(g) *Type A&B*; PGA=0.8*g* (h) *Type C*; PGA=0.8*g* (i) *Type D*; PGA=0.8*g*

Fig. 5 Distribution of hysteretic energy for the 9-storey frame, Nm × 10^6 (------- $E_{H,beams}$, ——— $E_{H,beams+columns}$)

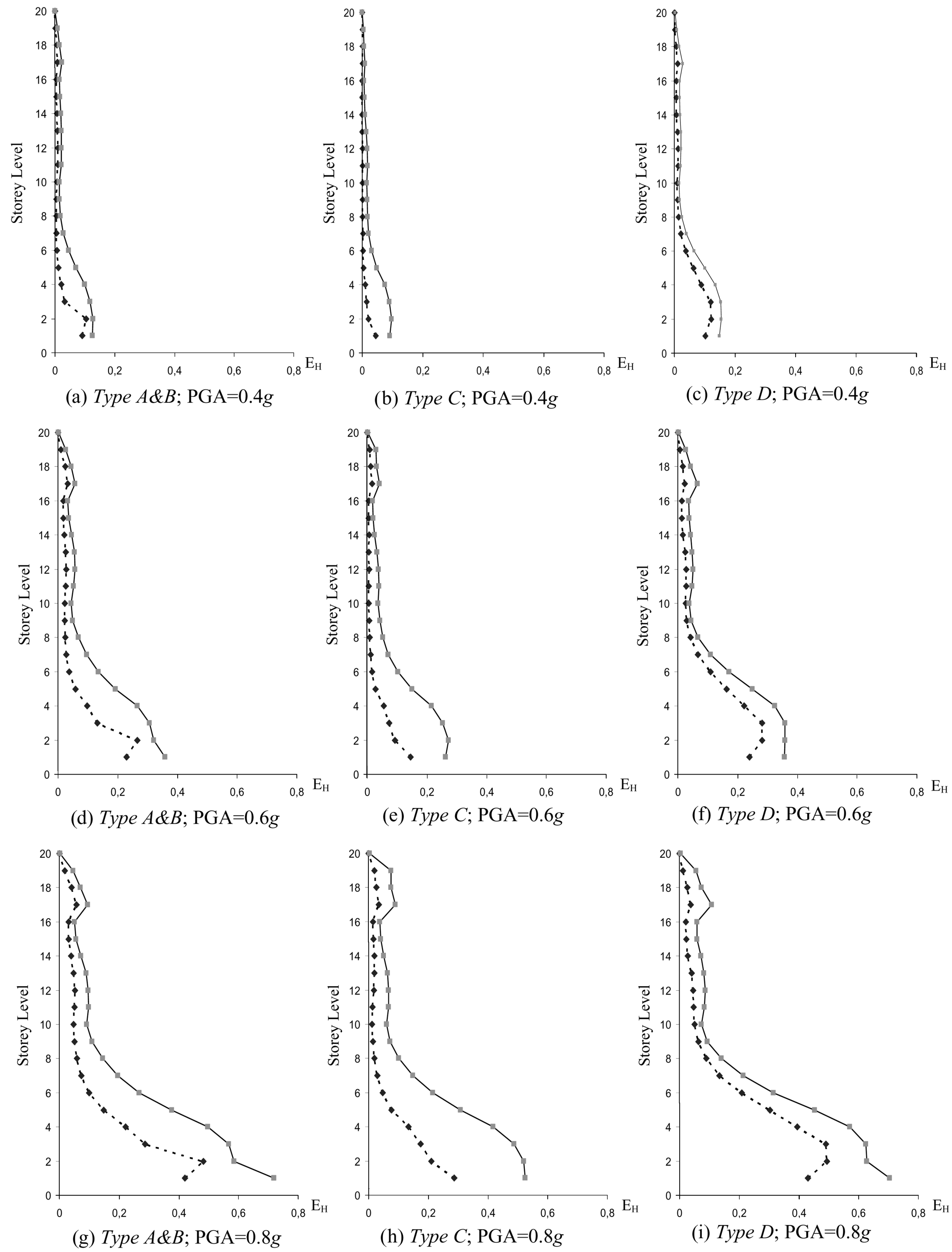

(a) *Type A&B*; PGA=0.4*g* (b) *Type C*; PGA=0.4*g* (c) *Type D*; PGA=0.4*g*

(d) *Type A&B*; PGA=0.6*g* (e) *Type C*; PGA=0.6*g* (f) *Type D*; PGA=0.6*g*

(g) *Type A&B*; PGA=0.8*g* (h) *Type C*; PGA=0.8*g* (i) *Type D*; PGA=0.8*g*

Fig. 6 Distribution of hysteretic energy for the 20-storey frame, Nm × 10^6 (------- $E_{H,beams}$, ——— $E_{H,beams+columns}$)

Table 1 $E_{H,beams}$ / $E_{H,beams+columns}$ for the 3-storey frame

Storey Level	PGA=0.4 g			PGA=0.6 g			PGA=0.8 g		
	Type A&B	Type C	Type D	Type A&B	Type C	Type D	Type A&B	Type C	Type D
1	0.85	0.89	0.80	0.74	0.81	0.72	0.68	0.73	0.66
2	0.99	1.00	0.99	1.00	1.00	0.99	1.00	1.00	0.99
3	0.99	1.00	0.98	1.00	1.00	0.99	1.00	1.00	0.99
Frame	0.92	0.94	0.89	0.86	0.91	0.85	0.84	0.87	0.83

Table 2 $E_{H,beams}$ / $E_{H,beams+columns}$ for the 9-storey frame

Storey Level	PGA=0.4 g			PGA=0.6 g			PGA=0.8 g		
	Type A&B	Type C	Type D	Type A&B	Type C	Type D	Type A&B	Type C	Type D
1	0.96	0.90	0.84	0.83	0.86	0.80	0.71	0.83	0.77
2	0.98	0.94	0.97	0.99	0.97	0.99	1.00	0.98	0.99
3	0.99	0.95	0.98	0.99	0.98	0.99	1.00	0.99	0.99
4	0.98	0.96	0.98	0.99	0.98	0.99	0.99	0.99	1.00
5	0.96	0.93	0.97	0.98	0.97	0.99	0.98	0.98	0.99
6	0.97	0.91	0.97	0.98	0.96	0.98	0.98	0.98	0.98
7	0.98	0.96	0.98	0.99	0.98	0.99	0.99	0.99	0.99
8	0.99	0.98	0.99	0.99	0.99	0.99	0.99	1.00	1.00
9	0.92	0.93	0.96	0.95	0.98	0.98	0.98	0.99	0.99
Frame	0.98	0.94	0.95	0.95	0.96	0.95	0.92	0.96	0.94

Table 2 shows the $E_{H,beams}$ to $E_{H,beams+columns}$ ratio at each storey of the 9-storey frame. The lowest $E_{H,beams}$ to $E_{H,beams+columns}$ ratio was 0.71 on *Type A&B* for PGA=0.8 g at the first storey and tended to decrease at the first storey as the EQ intensity increased. However, this ratio tended to increase at the other stories as the EQ intensity increased. At the other stories, this ratio varied from 0.91 to 1.00, i.e., only a small portion of the E_H was dissipated by the columns at the other stories. In overall, this ratio was in the range of 0.92 and 0.98 for the 9-storey frame. As in the case of the 3-storey frame, this should not let misinterpret the results, because for the 9-storey frame as well, the base of the first storey columns dissipated most of the E_H. This ratio was the highest for *Type A&B* for PGA=0.4 g, while it was the lowest for *Type D*. However, for PGA=0.6 g and 0.8 g, it was the highest at the first storey for *Type C* and the lowest for *Type A&B*. At the other stories, there was no significant difference for PGA = 0.6 g and 0.8 g. For PGA = 0.4 g, this ratio was approximately only a few percent lower for *Type C* than for *Type A&B* and *D*.

Table 3 shows the $E_{H,beams}$ to $E_{H,beams+columns}$ ratio at each storey of the 20-storey frame. The smallest $E_{H,beams}$ to $E_{H,beams+columns}$ ratio was 0.02 for *Type C* for PGA = 0.4 g at the twentieth storey. This ratio tends to increase as the soil softens. This ratio tended to decrease as the storey level increased, i.e., the columns participated the dissipation of the E_H far too much at the upper stories compared to bottom stories. However, most of the E_H was dissipated at the bottom stories. Since, this is only a ratio and does not give any clue as to the magnitude of the $E_{H,beams}$ or $E_{H,beams+columns}$, this ratio's being high at the upper storey levels should be meaningful if the E_H demands were compared only relatively. This ratio varied from 0.49 and 0.73 at the first storey. It tended to decrease as the EQ intensity increased at the first storey, but to increase at the others stories. This ratio was in the range of 0.02 and 0.83 at the other

Table 3 $E_{H,beams}$ / $E_{H,beams+columns}$ for the 20-storey frame

Storey Level	PGA=0.4 g			PGA=0.6 g			PGA=0.8 g		
	Type A&B	Type C	Type D	Type A&B	Type C	Type D	Type A&B	Type C	Type D
1	0.73	0.49	0.68	0.64	0.55	0.67	0.58	0.55	0.61
2	0.82	0.22	0.78	0.83	0.34	0.79	0.82	0.40	0.79
3	0.28	0.17	0.78	0.43	0.29	0.79	0.51	0.36	0.79
4	0.22	0.13	0.66	0.37	0.25	0.68	0.45	0.32	0.69
5	0.16	0.10	0.62	0.30	0.19	0.65	0.39	0.25	0.67
6	0.16	0.10	0.58	0.27	0.16	0.64	0.37	0.22	0.66
7	0.18	0.12	0.55	0.30	0.15	0.62	0.38	0.20	0.63
8	0.26	0.12	0.58	0.36	0.16	0.64	0.40	0.20	0.65
9	0.36	0.10	0.62	0.45	0.15	0.67	0.47	0.19	0.68
10	0.45	0.08	0.64	0.51	0.14	0.69	0.52	0.19	0.68
11	0.45	0.09	0.60	0.50	0.14	0.59	0.51	0.20	0.57
12	0.44	0.07	0.58	0.49	0.15	0.54	0.53	0.25	0.52
13	0.41	0.05	0.53	0.48	0.16	0.51	0.54	0.32	0.49
14	0.32	0.07	0.33	0.48	0.24	0.38	0.54	0.38	0.39
15	0.28	0.10	0.33	0.47	0.29	0.35	0.57	0.40	0.39
16	0.30	0.10	0.37	0.52	0.30	0.35	0.62	0.39	0.36
17	0.38	0.22	0.37	0.56	0.38	0.36	0.61	0.38	0.35
18	0.38	0.23	0.38	0.55	0.39	0.39	0.59	0.34	0.36
19	0.31	0.28	0.27	0.35	0.30	0.25	0.39	0.25	0.22
20	0.27	0.02	0.18	0.33	0.11	0.15	0.31	0.19	0.18
Frame	0.43	0.20	0.65	0.50	0.30	0.66	0.53	0.35	0.65

stories, i.e., a significant portion of the E_H was dissipated by the columns at the other stories. In overall, this ratio varied from 0.20 to 0.66 for the 20-storey frame. It was clear from Table 3 to say that the columns in the 20-storey frame exceeded the elastic range and dissipated a significant portion of the E_H for any soil type and EQ intensity.

For the 3-storey frame, the highest $E_{H,beams}$ demand occurred for *Type D*. For PGA=0.4 g, there was no significant difference in $E_{H,beams}$ for *Type A&B* and *C*. However, the increase in E_H was 35% for *Type D* with respect to *Type A&B* and *C* (Figs. 4(a), (b), and (c)). For PGA=0.8 g, the $E_{H,beams}$ increased about 10% and 20% for Type C and Type D with respect to Type A&B (Figs. 4(g), (h), and (i)). When PGA was scaled from 0.4 g to 0.8 g, the $E_{H,beams}$ demands increased approximately 5 times for all soil types. The highest increase was at the roof level (6.5 times) (Fig. 4).

For the 9-storey frame, the highest $E_{H,beams}$ demand occurred for *Type A&B*, while the lowest occurred for *Type C*. For PGA=0.4 g, the $E_{H,beams}$ demand increased about 3.9 and 1.58 times for *Type A&B* with respect to *Type C* and *Type D* at the roof level, while it increased 5.3 and 2.5 times at the first storey level (Figs. 5(a), (b), and (c)). For PGA=0.8 g, the increase for *Type A&B* was only about 1.3 and 1.4 times at the roof level, while it was 4.3 and 2.3 times at the first storey level (Figs. 5(g), (h), and (i)). When PGA was scaled from 0.4 g to 0.8 g, the $E_{H,beams}$ demands increased about 4.8, 5.7, and 5.3 times at the roof level for Type A&B, C, and D, respectively, while it increased about 5.1, 14.8, and 5.73 times at the first storey level.

For 20-story frame, the highest $E_{H,beams}$ demand occurred for *Type D*, while the lowest occurred for *Type C*. For PGA=0.4 g, the $E_{H,beams}$ demand increased about 1.3 and 47 times for *Type D* with respect to *Type A&B* and *Type C* at the roof level, while it increased 1.1 and 2.3 times at the first storey level (Figs. 6(a), (b), and (c)). For PGA=0.8 g, the $E_{H,beams}$ demand decreased about 10% for *Type D* with respect to *Type A&B* and *Type C*, while it increased about 1.3 times at the roof level. At the first storey level, the $E_{H,beams}$ demand increased about 1.02 and 1.5 times for *Type D* with respect to *Type A&B* and *Type C* (Figs. 6(g), (h), and (i)). When PGA was scaled from 0.4 g to 0.8 g, the $E_{H,beams}$ demands increased about 4.6, 6.4, and 4.3 times at the first storey level for *Types A&B, C*, and *D*, respectively, while it increased about 4.7, 100.0, and 3.2 times at the roof level. The increase of 47 and 100 times on *Type C* for PGA=0.4 g and 0.8 g, respectively, should not mislead due to their being so small.

4. Conclusions

This study has attempted to identify the hysteretic energy distribution throughout the height of regular steel moment resisting frames with respect to soil type and EQ intensity. The main conclusions obtained from this study and some recommendations for further studies are summarized below.

(1) Hysteretic energy is not a constant value and depends significantly on the properties of the structure and on the EQGM properties.
(2) Hysteretic energy demand decreases from the bottom stories to the upper stories. The decrease is quite significant, especially, for medium- and high-rise structures.
(3) Soil type and earthquake intensity have significant effects on the hysteretic energy input to the structure. For low-rise and high-rise structures used in this study (3- and 20-storey frames), the highest hysteretic energy demand occurred on soft soils (*Type D*). However, for the medium-rise structure (9-storey frame), the highest hysteretic energy demand occurred on *Type A&B*.
(4) For 9- and 20-storey frames, there was almost no E_H demand at the roof levels at all.
(5) Hysteretic energy demands might get higher values at the middle stories with respect to the nearby up and bottom stories.
(6) Non-linear dynamic time history analysis is used in this study. However, it is necessary to develop simpler methods for predicting the hysteretic energy demand in SDOF systems to be used in performance-based earthquake resistant design.
(7) This study is carried out on regular steel moment resisting frames. The variation of hysteretic energy for structures with different configurations should be further studied.
(8) If the hysteretic energy is estimated by some means, then this energy can be dissipated through the height of the structure approximately.
(9) Knowing the hysteretic energy demand is not enough to design a structure or component, the hysteretic energy dissipation capacity should also be known.

References

AISC-LRFD (1999), *Load and Resistance Factor Design*, American Institute of Steel Construction, Chicago.
Akiyama, H. (1985), *Earthquake-Resistant Limit-State Design for Buildings,* University of Tokyo Press.
Bertero, V. V. and Teran-Gilmore, A. (1994), "Use of energy concepts in earthquake-resistant analysis and design: Issues and future directions", *Advances in Earthquake Engineering Practice, Short Course in Structural Engineering, Architectural and Economic Issues*, University of California, Berkeley.

Bertero, R. D. and Bertero, V. V. (1999), "Redundancy in earthquake resistant design", *J. Struct. Eng.,* **125**(1), 81-88.

Bruneau, B. and Wang, N. (1996), "Some aspects of energy methods for the inelastic seismic response of ductile SDOF structures", *Eng. Struct.*, **18**(1), 1-12.

Choi, B. J. (2004), "Hysteretic energy response of steel moment resisting frames with vertical mass irregularities", *Structural Design of Tall and Special Buildings*, **3**, 123-144.

Chopra, A. K. (2000), *Dynamics of Structures: Theory and Applications to Earthquake Engineering*, Prentice-Hall Inc, New Jersey.

Fajfar, P. and Vidic, T. (1989), "Seismic demand in medium- and long-period structures", *Earthq. Eng. Struct. Dyn.,* **18**, 513-537.

Housner, G. W. (1956), "Limit design of structures to resist earthquakes", *Proc. of the First World Conf. on Earthquake Engineering*, Berkeley, California, 5-1-5-13.

Kuvamura, H. and Galambos, T. V. (1989), "Earthquake load for structural reliability", *J. Struct. Eng*, **115**(6), 1446-1463.

Kuwamura, H., Akiyama, H. and Kirino, Y. (1992), "Prediction of earthquake energy input from smoothed Fourier amplitude spectrum", *J. Const. Eng. Transact. of AIJ*, **442**, 53-60.

Ohtori, Y., Christenson, R.E., Spencer, Jr. and Dyke, S.J. (2000), "Benchmark control problems for seismically excited nonlinear buildings", *http://www.nd.edu/~quake/, Notre Dame University*, Indiana.

Prakash, V., Powell, G. H. and Campbell, S. (1993), *DRAIN-2DX: Base Program Description and User Guide, Version 1.10,* Rep. No. UCB/SEMM-93/17, University of California, Berkeley.

Reyes-Salazar, A. and Haldar, A. (2000), "Dissipation of energy in steel frames with PR connections", *Struct. Eng. Mech.,* **9**(3), 241-256.

Reyes-Salazar, A. and Haldar, A. (2001a), "Energy dissipation at PR frames under seismic loading", *J. Struct. Eng.*, **127**(5), 588-592.

Reyes-Salazar, A. and Haldar, A. (2001b), "Seismic response and energy dissipation in partially restrained and fully restrained steel frames: An analytical study", *Steel and Composite Structures*, **1**(4), 459-480.

Sari, A. (2003), "Energy consideration in ground motion attenuation and probabilistic seismic hazard studies", Ph.D. Thesis, Department of Civil Engineering, University of Texas at Austin.

Shen, J. and Akbas, B. (1999), "Seismic energy demand in steel moment frames", *J. Earthq. Eng.*, **3**(4), 519-559.

Tso, W. K., Zhu, T. J. and Heidebracht, A. C. (1993), "Seismic energy demands on reinforced concrete moment-resisting frames", *Earthq. Eng. Struct. Dyn.*, **22**, 533-545.

Uang, C. M. and Bertero, V. V. (1990), "Evaluation of seismic energy in structures", *Earthq. Eng. Struct. Dyn.,* **19**, 77-90.

Vision-2000 (1995), *Structural Engineering Association of California (SEAOC).*

Zahrah, T. F. and Hall, W. J. (1984), "Earthquake energy absorption in simple structures", *J. Struct. Eng.*, **110**(8), 1757-1773.

CC